

# Cold nuclear matter effects on the color singlet $J/\psi$ production in $dAu$ collisions at energies available at the BNL Relativistic Heavy Ion Collider

Ze-Fang Jiang,<sup>1</sup> Sheng-Qin Feng,<sup>1,2,4,\*</sup> Zhong-Bao Yin,<sup>2,3</sup> Ya-Fei Shi,<sup>1</sup> and Xian-Bao Yuan<sup>1</sup><sup>1</sup>College of Science, China Three Gorges University Yichang 443002, China<sup>2</sup>Key Laboratory of Quark and Lepton Physics (Huazhong Normal University), Ministry of Education, Wuhan 430079 China<sup>3</sup>Institute of Particle Physics, Central China Normal University, Wuhan 430079, China<sup>4</sup>School of Physics and Technology, Wuhan University, Wuhan 430072, China

(Received 26 August 2014; revised manuscript received 4 November 2014; published 26 November 2014)

We use a modified DKLMT model (M-DKLMT) to study the cold nuclear matter (CNM) effects on the color singlet  $J/\psi$  production in  $dAu$  collisions at RHIC. The cold nuclear effect of dipole-nucleus interactions has been investigated by introducing a nuclear geometric effect function  $f(\xi)$  to study the nuclear geometry distribution effect in relativistic heavy-ion collisions. The dependencies of nuclear modification factors ( $R_{dA}$ ) on rapidity and centrality are studied and compared to experimental data. It is found that the M-DKLMT model can well describe the experimental results at both forward- and midrapidity regions in  $dAu$  collisions at RHIC.

DOI: 10.1103/PhysRevC.90.054913

PACS number(s): 25.75.Dw, 14.40.Pq, 14.70.Dj

## I. INTRODUCTION

Heavy quark production in high-energy nuclear collisions has been a focus of interest for many years. Heavy quarks are essential probes of the evolution of the medium created in heavy-ion collisions since they are produced predominantly in the early stage of nuclear collisions [1]. Heavy-quark production in  $pp$  collisions was studied not only to test the perturbative quantum chromodynamics but also to serve as a baseline for studying heavy-ion collisions [2–4]. Although suppression of high  $p_T$  particles was predicted as an effect of parton energy loss in the hot dense medium created in relativistic heavy-ion collisions [5–7], it is difficult to account for the comparable suppression of heavy flavors to that of light flavors solely with hot nuclear matter effects [8]. To understand comprehensively the parton energy-loss mechanism in hot dense medium, it is essential to explore fully the underlying cold nuclear matter (CNM) effects.

While measurement of heavy-flavor production in elementary collisions is crucial to test the validity of the current theoretical framework and for inputs to phenomenological models to describe heavy-flavor production in nucleus-nucleus collisions, control experiments with  $pA$  or  $dA$  collisions allow us to probe those CNM effects. These include modifications of the parton distribution function (PDF) and  $k_T$  broadening, with minimal impact from the hot nuclear medium. Because heavy quarks are produced primarily by gluon fusion at RHIC, modification of the gluon density in nucleus can be observed in charm and bottom production rates [9,10].

Based on the McLerran-Venugopalan (MV) model [11], Dominguez, Kharzeev, Levin, Mueller, and Tuchin (DKLMT) proposed a model [12] to analyze the gluon saturation effects on the color singlet  $J/\psi$  productions in  $dA$  and  $AA$  collisions at RHIC energies [13–16]. The DKLMT model [12] assumes that  $c\bar{c}$  pair in a color-octet state propagates through the nucleus and becomes color singlet inside the nucleus. In the large  $N_c$  approximation further color conversions of the  $c\bar{c}$  state

are suppressed and thus can be neglected. Therefore, in this case the  $c\bar{c}$  experiences the last inelastic interaction inside the nucleus after which it rescatters only elastically. Additionally, the DKLMT model treats the  $J/\psi$  wave function accurately with parameters determined from a fit to the exclusive  $J/\psi$  production in deep inelastic scattering.

Based on the DKLMT model, we propose a new form of cold nuclear matter effect on the color singlet  $J/\psi$  production mechanism in order to describe  $dA$  experimental data at RHIC. This Modified DKLMT model (M-DKLMT model) can describe the centrality and rapidity dependencies of nuclear modification factor ( $R_{dA}$ ) for  $J/\psi$  productions in  $dAu$  collisions at RHIC.

This paper is organized as follows: Sec. II introduces the M-DKLMT model including the nuclear modification effects in  $dAu$  collisions; Sec. III is dedicated to the description of the numerical calculation performed with DHJ model [17] for the dipole scattering amplitude, and the calculation results are then compared with the experimental data at RHIC. The conclusions are summarized in Sec. IV.

## II. THE M-DKLMT MODEL AND NUCLEAR MODIFICATION EFFECT

The DKLMT model [12] contains three distinct assumptions.

(i) In order to study  $J/\psi$  production in high-energy  $pA$  (or  $dA$ ) collisions, DKLMT model argued that  $J/\psi$  production in relativistic heavy-ion collisions should take into account the gluon saturation and color glass condensate effects. The  $J/\psi$  production cross section in high-energy  $pA$  (or  $dA$ ) collisions can be written in the factorized form:

$$\frac{d\sigma_{pA \rightarrow J/\psi X}}{db^2 dy} = x_1 G(x_1, m_c^2) \frac{d\sigma_{gA \rightarrow J/\psi X}}{db^2}, \quad (1)$$

where a simple ansatz for the gluon distribution [18] encoding the saturation [19] is given as follows:

$$x_1 G(x_1, m_c^2) = \begin{cases} \frac{K}{\alpha_s(Q_s)} m_c^2 (1-x_1)^4, & m_c < Q_s(x_1) \\ \frac{K}{\alpha_s(Q_s)} Q_s^2 (1-x_1)^4, & m_c > Q_s(x_1) \end{cases}, \quad (2)$$

\* fengsq@ctgu.edu.cn

with  $x_1 = (m_c/\sqrt{s})e^y$ ,  $m_c$  is the charm quark mass and  $\sqrt{s}$  the collision energy in the center of mass system, the normalization factor  $K$ , and  $\alpha_s(Q_s)$  are determined by a fit to  $pp$  data and  $d$ -Au data at RHIC.

(ii) In order to study  $\frac{d\sigma_{gA \rightarrow J/\psi X}}{db^2}$ , DKLMT used a well-developed phenomenology  $\gamma A$  theory by stating a  $\gamma p$  scattering,

$$\frac{d\sigma_{\gamma A \rightarrow J/\psi X}}{dt} = \frac{1}{16} |A_{\gamma p \rightarrow J/\psi p}|^2, \quad (3)$$

with

$$A_{\gamma p \rightarrow J/\psi X}(x, \Delta) = \int d^2b e^{-i\Delta \cdot b} \int_0^1 dz \int \frac{d^2r}{4\pi} (\Psi_{J/\psi}^* \Psi_\gamma) 2i [1 - S(x, \mathbf{r}, \mathbf{b})], \quad (4)$$

where  $t = -\Delta^2$  is the momentum transfer, and  $\Psi_{J/\psi}^* \Psi_\gamma = \Phi_\gamma(\mathbf{r}, z)$  with

$$\begin{aligned} \phi_\gamma(\mathbf{r}, z) = & \frac{2}{3} e \frac{N_c}{\pi} \left\{ m_c^2 K_0(m_c \mathbf{r}) \phi_T(\mathbf{r}, z) \right. \\ & \left. - [z^2 + (1-z)^2] m_c K_1(m_c \mathbf{r}) \partial_r \phi_T(\mathbf{r}, z) \right\}, \end{aligned} \quad (5)$$

where

$$\phi_T(r, z) = N_T z(1-z) \exp\left[-\frac{r^2}{2R_T^2}\right], \quad (6)$$

and where  $N_T = 1.23$ ,  $R_T^2 = 6.5 \text{ GeV}^{-2}$  [19].

By integrating over  $\Delta$ , Eq. (3) can be given as

$$\begin{aligned} \frac{d\sigma_{\gamma A \rightarrow J/\psi A'}}{d^2b} = & \int_0^1 dz \int \frac{d^2r}{4\pi} \Phi_\gamma(\mathbf{r}, z) \\ & \times \int_0^1 dz' \int \frac{d^2r'}{4\pi} \Phi_\gamma^*(\mathbf{r}', z') [1 - S^*(r')] \\ & \times [1 - S(r)]. \end{aligned} \quad (7)$$

According to the McLerran-Venugopalan model [11], the  $S$  factors are given by

$$S(r) \simeq \exp\left[-\frac{1}{8} Q_s^2 r^2\right], \quad (8)$$

where  $Q_s$  is the gluon saturation scale function and its detailed form will be given in Eq. (19).

(iii) DKLMT established the dipole-A interaction picture as shown in Fig. 1. The  $J/\psi$  formed from  $c\bar{c}$  is a color singlet. It is the particular dipole-nucleon inelastic collision that converts the adjoint representation to a color singlet in the large- $N_c$  approximation. The longitudinal coordinate  $\xi$  (as shown in Fig. 1 the distance from the front of the nucleus) indicates the point where the particular inelastic interaction takes place. In order to keep the singlet intact, it is clear that later interactions, occurring after the  $c\bar{c}$  pair is in a singlet state, are purely elastic.

The interaction at  $\xi$ , responsible for the transition from a color octet state to a color singlet state, can involve the antiquark in both the amplitude and the conjugate amplitude. Under the MV model evaluation employed here, the given

interaction probability factor is

$$\frac{Q_s^2 \mathbf{r} \cdot \mathbf{r}'}{4T(b)} d\xi. \quad (9)$$

$T(b)$  depicts the nuclear thickness [20] at given impact parameter  $b$ ,

$$T(b) = 2\sqrt{R^2 - b^2} \theta(R - b), \quad (10)$$

where  $R$  is the radius of target nucleus and  $\theta$  is the step function. The interactions occurring before  $\xi$  can be taken into account. With dipole separation  $(\mathbf{r} - \mathbf{r}')/2$ , each of these pieces can be treated as a dipole interaction with the nucleus. This given the combined factor

$$e^{-\frac{1}{16} Q_s^2 (\mathbf{r} - \mathbf{r}')^2 [\xi/T(b)]}, \quad (11)$$

where the  $\xi/T(b)$  factor is for these interactions before the last inelastic interaction at longitudinal coordinate  $\xi$ . As follows, we will provide these interactions after the last inelastic interactions. The combined factor are given as follows:

$$e^{-\frac{1}{8} Q_s^2 (\mathbf{r}^2 + \mathbf{r}'^2) [1 - \xi/T(b)]}. \quad (12)$$

The cross section of  $gA \rightarrow J/\psi X$  was given by Ref. [12]:

$$\begin{aligned} \frac{d\sigma_{gA \rightarrow J/\psi X}}{d^2b} = & \int_0^1 dz \int \frac{d^2r}{4\pi} \Phi(\mathbf{r}, z) \int_0^1 dz' \int \frac{d^2r'}{4\pi} \Phi^*(\mathbf{r}', z') \\ & \times \int_0^{T(b)} d\xi \frac{\mathbf{r} \cdot \mathbf{r}'}{4T(b)} \exp\left\{-\frac{1}{16} Q_s^2 (\mathbf{r} - \mathbf{r}')^2 \right. \\ & \left. \times \left(\frac{\xi}{T(b)}\right) - \frac{1}{8} Q_s^2 (\mathbf{r}^2 + \mathbf{r}'^2) \left(1 - \frac{\xi}{T(b)}\right)\right\}. \end{aligned} \quad (13)$$

After this consideration, the cross-section distribution of  $pA \rightarrow J/\psi X$  was provided [12] as follows:

$$\begin{aligned} \frac{d\sigma_{pA \rightarrow J/\psi X}}{dy d^2b} = & x_1 G(x_1, m_c^2) \int_0^1 dz \int \frac{d^2r}{4\pi} \Phi(\mathbf{r}, z) \\ & \times \int_0^1 dz' \int \frac{d^2r'}{4\pi} \Phi^*(\mathbf{r}', z') \\ & \times \frac{4\mathbf{r} \cdot \mathbf{r}'}{(\mathbf{r} + \mathbf{r}')^2} \left[ e^{-\frac{1}{16} Q_s^2 (\mathbf{r} - \mathbf{r}')^2} - e^{-\frac{1}{8} Q_s^2 (\mathbf{r}^2 + \mathbf{r}'^2)} \right], \end{aligned} \quad (14)$$

where

$$\begin{aligned} \phi(\mathbf{r}, z) = & \frac{g}{\pi \sqrt{2} N_c} \left\{ m_c^2 K_0(m_c \mathbf{r}) \right. \\ & \left. - [z^2 + (1-z)^2] m_c K_1(m_c \mathbf{r}) \partial_r \phi_T(\mathbf{r}, z) \right\}, \end{aligned} \quad (15)$$

in which  $K_0$  and  $K_1$  are the modified Bessel functions.

According to DKLMT and MV model [shown at Eqs. (9) and (14)], the productions of  $J/\psi$  in  $pA$  interactions are independent of the longitudinal coordinate  $\xi$ , which means that at different location of  $\xi$  the production probability is the same. We argued that the productions of  $J/\psi$  in relativistic heavy-ion interactions should rely on the longitudinal coordinate  $\xi$  and impact parameter  $b$ . When  $b \ll R$ , the dipole-nucleus collisions propagate through the whole nuclear thickness, the

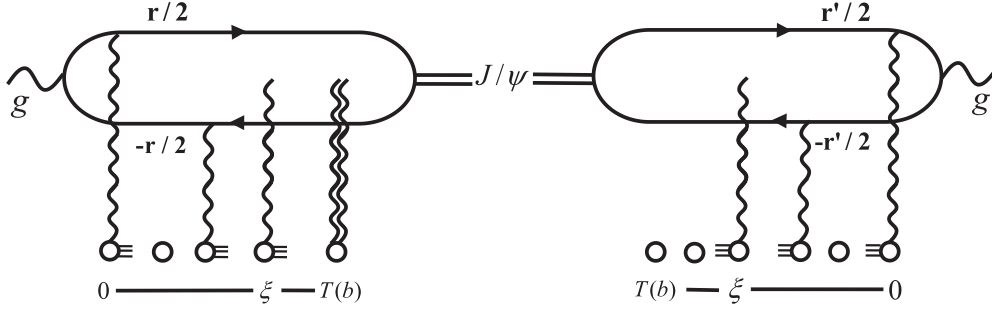


FIG. 1. A sketch diagram for  $gA \rightarrow J/\psi$ . The longitudinal coordinate  $\xi$  is the point where the last inelastic interaction takes place.

probability for the inelastic scattering is thus proportional to the longitudinal coordinate. This implies that the nuclear geometric effects play an important role to the  $J/\psi$  production suppression. At  $b \approx R$ ,  $J/\psi$  production in  $dAu$  collisions becomes similar to that in  $pp$  collisions, the cold nuclear geometric effect is believed to be small and can be neglected.

In order to study the effects of dipole cold nuclear matter interaction at different point  $\xi$  at different impact parameters inside the nucleus, we thus introduce a nuclear geometric effect function  $f(\xi)$  of the interaction at  $\xi$  to account for the position dependence of the probability to form the  $J/\psi$  under the dipole-nucleus collisions as following:

$$\frac{Q_s^2 \mathbf{r} \cdot \mathbf{r}'}{4T(b)} f(\xi) d\xi. \quad (16)$$

After introducing the nuclear geometric effect function  $f(\xi)$  to take into account the different probability of inelastic interaction at different location  $\xi$ , the cross section for  $J/\psi$  production in  $pA$  collisions becomes a function of the nuclear thickness function. The nuclear geometric effect function  $f(\xi)$  is not a flat distribution of  $\xi$  in our assumption; the smaller the magnitude of  $\xi$ , the larger the value of  $f(\xi)$ . The form of the nuclear matter coherent function is assumed to be a likely Gaussian form:

$$f(\xi) = \alpha e^{-\beta \left(\frac{\xi}{T(b)}\right)^2}, \quad (17)$$

where  $\alpha$  is a normalization factor, and  $\beta$  is an adjustable parameter, which can be determined from experimental data.

In order to calculate the nuclear modification factor  $R_{dA}$  at different centrality and at different rapidity regions, it is necessary to describe the nuclear geometry feature properly. The relation between impact parameter  $b$  and the number of participant ( $N_{\text{part}}$ ) in  $dAu$  collisions is already derived in Ref. [21] and given by

$$b = R_{\text{Au}} \sqrt{1 - \frac{(N_{\text{part}} - 2)^2}{A^2 \left[1 - \left(1 - \frac{R_d^2}{R_{\text{Au}}^2}\right)^{3/2}\right]^2}}, \quad (18)$$

where  $A$  is the number of target nucleon of gold,  $R_{\text{Au}}$  the radius of target gold nucleus, and  $R_d$  the radius of the projectile deuterium nucleus.

The DHJ model [17] has improved the KKT model [22,23] by taking into account the change in the anomalous dimension of the gluon distribution function due to the presence of the saturation boundary [24] and also some higher-order effects.

The DHJ model performs the numerical calculations of the dipole scattering amplitude [17] as follows:

$$N_A(\mathbf{r}, y) = 1 - \exp\left\{-\frac{1}{4}(r^2 Q_s^2)^\gamma\right\}. \quad (19)$$

The gluon saturation scale is given by

$$Q_s^2 = \Lambda^2 A^{1/3} e^{\lambda y} = 0.13 \text{ GeV}^2 e^{\lambda y} N_{\text{coll}}, \quad (20)$$

and the parameters  $\gamma$  is the anomalous dimension

$$\gamma = \gamma_s + (1 - \gamma_s) \frac{\ln(m^2/Q_s^2)}{\lambda Y + \ln(m^2/Q_s^2) + d\sqrt{Y}}, \quad (21)$$

where  $\gamma_s = 0.628$  is implied by theoretical arguments [25] and  $d = 1.2$ ,  $Y = \ln(1/x)$ ,  $x = me^{-y}\sqrt{s}$ ,  $\Lambda = 0.6 \text{ GeV}$ , and  $\lambda = 0.3$  are fixed by DIS data [26,27]. Besides the DHJ model, another model [28] also used the anomalous dimension of the gluon distribution function to study dipole scattering amplitude.

After the consideration of geometric modification of the DKLMT model, we provide the cross section as follows:

$$\begin{aligned} \frac{d\sigma_{gA \rightarrow J/\psi X}}{d^2b} &= \int_0^1 dz \int \frac{d^2r}{4\pi} \Phi(\mathbf{r}, z) \int_0^1 dz' \int \frac{d^2r'}{4\pi} \Phi^*(\mathbf{r}', z') \\ &\times \int_0^{T(b)} d\xi \frac{\mathbf{r} \cdot \mathbf{r}'}{4T(b)} \exp\left\{-\beta \left(\frac{\xi}{T(b)}\right)^2\right. \\ &\quad \left.- \frac{1}{16} Q_s^2(\mathbf{r} - \mathbf{r}')^2 \left(\frac{\xi}{T(b)}\right)\right. \\ &\quad \left.- \frac{1}{8} Q_s^2(\mathbf{r}^2 + \mathbf{r}'^2) \left(1 - \frac{\xi}{T(b)}\right)\right\}. \end{aligned} \quad (22)$$

The cross section of  $pA \rightarrow J/\psi X$  is given by

$$\begin{aligned} \frac{d\sigma_{pA \rightarrow J/\psi X}}{dy d^2b} &= x_1 G(x_1, m_c^2) \frac{\alpha}{2} \sqrt{\frac{\pi}{\beta}} \int_0^1 dz \int \frac{d^2r}{4\pi} \Phi(\mathbf{r}, z) \\ &\times \int_0^1 dz' \int \frac{d^2r'}{4\pi} \Phi^*(\mathbf{r}', z') \frac{Q_s^2 \mathbf{r} \cdot \mathbf{r}'}{4} \\ &\times e^{-\frac{1}{8} Q_s^2(\mathbf{r}+\mathbf{r}')^2 + \frac{1}{32\beta} Q_s^4(\mathbf{r}+\mathbf{r}')^4} \left\{ \left( \Phi\left(\frac{Q_s^2(\mathbf{r}+\mathbf{r}')^2}{32\sqrt{\beta}}\right) \right. \right. \\ &\quad \left. \left. + \Phi\left[\sqrt{\beta} \left(1 - \frac{Q_s^2(\mathbf{r}+\mathbf{r}')^2}{32\beta}\right)\right] \right\}, \end{aligned} \quad (23)$$

where  $\Phi(\mu) = \int_0^\mu e^{-x^2} dx$  is the error function. Compared with Eq. (14) given by the DKLMT model, Eq. (23) has a different

form by introducing the Gaussian function  $f(\xi)$  of nuclear geometrical effect. One can find that the cross section of  $pA \rightarrow J/\psi X$  is sensitive to the Gaussian form and the parameter  $\beta$ . By fit, the experimental results of RHIC, the given  $\beta$  is 9.

After consideration of the DHJ model, the cross section is given as follows:

$$\begin{aligned} & \frac{d\sigma_{pA \rightarrow J/\psi X}}{dyd^2b} \\ &= x_1 G(x_1, m_c^2) \frac{\alpha}{2} \sqrt{\frac{\pi}{\beta}} \int_0^1 dz \int \frac{d^2r}{4\pi} \Phi(\mathbf{r}, z) \\ & \times \int_0^1 dz' \int \frac{d^2r'}{4\pi} \Phi^*(\mathbf{r}', z') \frac{(Q_s \mathbf{r})^\gamma \cdot (Q_s \mathbf{r}')^\gamma}{4} \\ & \times \exp \left\{ -\frac{1}{8} [Q_s(\mathbf{r} + \mathbf{r}')^{2\gamma}] + \frac{1}{32^2 \beta} [Q_s \cdot (\mathbf{r} + \mathbf{r}')^{4\gamma}] \right\} \\ & \times \left\{ \Phi \left( \frac{[Q_s(\mathbf{r} + \mathbf{r}')^{2\gamma}]}{32\sqrt{\beta}} \right) + \Phi \left[ \sqrt{\beta} \left( 1 - \frac{[Q_s(\mathbf{r} + \mathbf{r}')^{2\gamma}]}{32\beta} \right) \right] \right\}. \end{aligned} \quad (24)$$

### III. CALCULATIONS AND RESULTS

In this section, we calculate nuclear modification factor and compare the results to the experimental measurements in 200 GeV  $dAu$  collisions at RHIC [13–16]. To study the nuclear matter effect in  $dAu$  collisions, we recall the definition of nuclear modification factor (NMF),

$$R_{dA} = \frac{d\sigma_{J/\psi}^{dAu}/dy}{\langle N_{\text{coll}} \rangle d\sigma_{J/\psi}^{pp}/dy}, \quad (25)$$

where  $N_{\text{coll}}$  is the number of binary nucleon-nucleon collisions.

The NMF results of our M-DKLMT model in  $dAu$  collisions at RHIC are shown in Figs. 2, 3, and 4.

Figure 2 shows the dependencies of nuclear modification factors  $R_{dA}$  on the number of participants at different rapidity regions. One can find that when introducing the Gaussian geometric effect function  $f(\xi)$ , a strong suppression of  $R_{dA}$  at small  $N_{\text{part}}$  is shown in our M-DKLMT model. The results shown in Fig. 2 indicate that our M-DKLMT model describes the experimental data better than that of the DKLMT model, especially at the forward rapidity of  $1.2 < y < 2.2$ .

The rapidity dependencies of  $R_{dAu}$  for different collision centralities are shown in Fig. 3. Comparing with the results of DKLMT, we find that our M-DKLMT model results in a stronger suppression at midrapidity region. In addition, our M-DKLMT model describes the experimental data better than that of the DKLMT model, especially for the central collisions as shown in Fig. 3(a). When considering the nuclear geometric effect, we find that the nuclear thickness  $T(b)$  of central collisions is large, the nuclear medium effect is obvious, which can reflect one of the characteristics of cold nuclear geometric effects.

Figure 4 shows the rapidity dependencies of the nuclear modification factors for centrality of 0–100%. The solid line shows our calculation result and the dashed line is the result from the DKLMT model calculation. Comparing with the

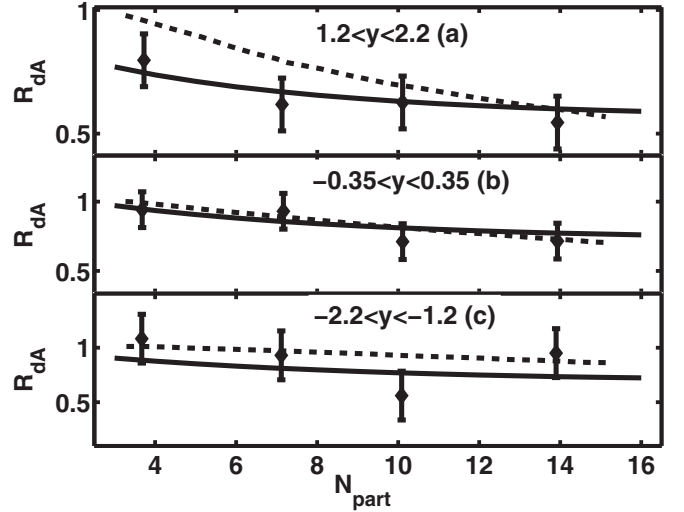


FIG. 2. The dependencies of nuclear modification factors  $R_{dA}$  on the number of participants at different rapidity regions: (a) for  $1.2 < y < 2.2$ , (b) for  $-0.35 < y < 0.35$ , and (c) for  $-2.2 < y < -1.2$ . The experimental results come from Refs. [13–16]. The solid lines are our calculation results and the dashed lines are the results from the DKLMT model.

DKLMT model, the M-DKLMT model calculation shows good agreement with experimental data.

### IV. CONCLUSIONS AND DISCUSSIONS

The studies of  $p(d)A$  collisions at different energies were motivated in order to understand cold nuclear matter effects [30–33]. These CNM effects can modify  $J/\psi$  production in  $pA$  collisions as compared to  $pp$  collisions where in both cases a QGP is believed to be absent. CNM effects that were often considered include nuclear modification of

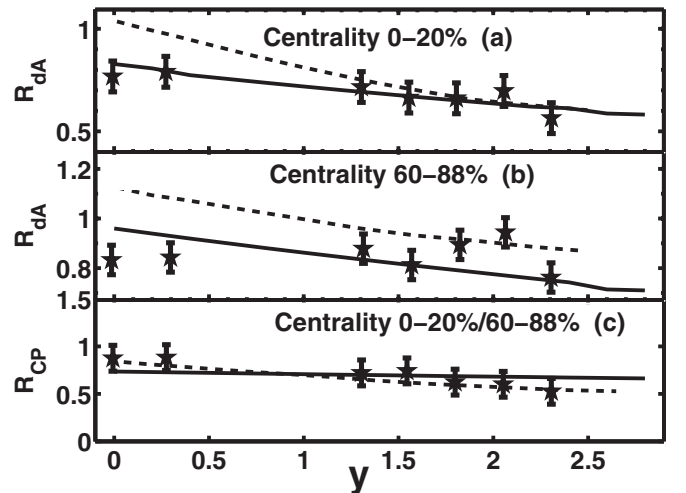


FIG. 3. The rapidity dependencies of  $R_{dAu}$  on different collision centralities: (a) 0–20%, (b) 60–88%, and (c) for  $R_{CP}$  the ratio of 0–20%/60–88%. The solid lines are our calculation results and the dashed lines are the results from the CGC model [29].

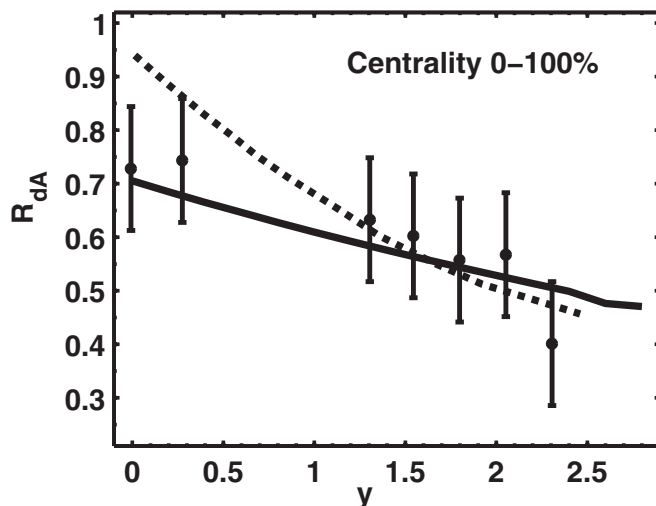


FIG. 4. The rapidity dependencies of nuclear modification factors for centrality of 0–100%. The solid line indicates our calculation result and the dashed line shows the result from the CGC model [33].

the parton distributions in nuclei (nPDFs), breakup of the  $J/\psi$  precursor state in the cold nucleus, parton transverse momentum broadening in traversing the cold nucleus, and initial state parton energy loss [30,31]. It has been hoped that CNM effects and hot matter effects can be factorized, so that CNM effects can be measured in  $p(d)A$  collisions and accounted for when analyzing heavy ion collisions data to extract hot dense medium effects.

Reference [34], a research of the production of heavy quarkonium states in high energy proton-nucleus collisions, systematically included both small  $x$  evolution and multiple scattering effects on heavy quark pair production within the

color glass condensate (CGC) framework. It was observed [34] that the production of color singlet heavy quark pairs is sensitive to both quadrupole and dipole Wilson line correlators, whose energy evolution is described by the Balitsky-JIMWLK equations. In contrast, the color octet channel is sensitive to dipole correlators alone. In a quasiclassical approximation, their results for the color singlet channel reduce to those of Dominguez *et al.* [12].

In this paper we developed a modified DKLMT model to describe the cold nuclear matter effects on the color singlet  $J/\psi$  productions in  $dAu$  collisions at RHIC. In order to describe the centrality and rapidity dependencies of nuclear modification factor ( $R_{dA}$ ) for  $J/\psi$  productions at RHIC, the nuclear geometric effect function  $f(\xi)$  and the relationship between impact parameter  $b$  and the number of participants ( $N_{\text{part}}$ ) in  $dAu$  collisions are introduced to the M-DKLMT model. The nuclear geometric effect function  $f(\xi)$  is mainly to account for the different interaction probability at different location  $\xi$ . It is realized that the nuclear geometric effect function  $f(\xi)$  is not uniform but has a larger value at smaller  $\xi$ .

One can find that the M-DKLMT model introduces a stronger suppression at small  $N_{\text{part}}$  and at midrapidity region by comparing with DKLMT model. The M-DKLMT model can describe the experimental data better than that of the DKLMT model, especially for the forward rapidity region  $1.2 < y < 2.2$  and for the central collisions.

#### ACKNOWLEDGMENTS

This work was supported by the National Natural Science Foundation of China (Grants No. 11475068 and No. 11247021), also by the Open innovation fund of the Ministry of Education of China under Grant No. QLPL2014P01.

- [1] T. Matusi and H. Satz, *Phys. Lett. B* **178**, 416 (1986).
- [2] S. Adler *et al.* (PHENIX collaboration), *Phys. Rev. D* **76**, 092002 (2007).
- [3] A. Adare *et al.* (PHENIX collaboration), *Phys. Rev. Lett.* **97**, 252002 (2006).
- [4] H. Agakishiev *et al.* (STAR collaboration), *Phys. Rev. D* **83**, 052006 (2011).
- [5] M. G. Mustafa, *Phys. Rev. C* **72**, 014905 (2005).
- [6] G. D. Moore and D. Teaney, *Phys. Rev. C* **71**, 064904 (2005).
- [7] H. van Hees, V. Greco, and R. Rapp, *Phys. Rev. C* **73**, 034913 (2006).
- [8] A. Adare *et al.* (PHENIX collaboration), *Phys. Rev. C* **86**, 024909 (2012).
- [9] K. J. Eskola, H. Paukkunen, and C. A. Salgado, *J. High Energy Phys.* **04** (2009) 065.
- [10] I. Helenius, K. J. Eskola, H. Honkanen, and C. A. Salgado, *J. High Energy Phys.* **07** (2012) 073.
- [11] L. McLerran and R. Venugopalan, *Phys. Rev. D* **49**, 3352 (1994).
- [12] F. Dominguez, D. E. Kharzeev, E. M. Levin, A. H. Mueller, and K. Tuchin, *Phys. Lett. B* **710**, 182 (2012).
- [13] A. Adare *et al.* (PHENIX collaboration), *Phys. Rev. C* **77**, 024912 (2008).
- [14] A. Adare *et al.* (PHENIX collaboration), *Phys. Rev. C* **79**, 059901(E) (2009).
- [15] S. Adler *et al.* (PHENIX collaboration), *Phys. Rev. Lett.* **96**, 012304 (2006).
- [16] S. Adler *et al.* (PHENIX collaboration), *Phys. Rev. Lett.* **98**, 232002 (2007).
- [17] A. Dumitru, A. Hayashigaki, and J. Jalilian-Marian, *Nucl. Phys. A* **770**, 57 (2006).
- [18] D. Kharzeev and E. Levin, *Phys. Lett. B* **523**, 79 (2001).
- [19] A. Dumitru, D. E. Kharzeev, E. M. Levin, and Y. Nara, *Phys. Rev. C* **85**, 044920 (2012).
- [20] C. Y. Wong, *Introduction to High-Energy Heavy-Ion Collisions* (World Scientific, Singapore, 1994), p. 262.
- [21] X. Cai, S. Q. Feng, Y. D. Li, C. B. Yang, and D. C. Zhou, *Phys. Rev. C* **51**, 3336 (1995).
- [22] D. E. Kharzeev, Y. Kovchegov, and K. Tuchin, *Phys. Lett. B* **599**, 23 (2004).
- [23] K. Tuchin, *Nucl. Phys. A* **798**, 61 (2008).
- [24] A. Muller and D. Triantafyllopoulos, *Nucl. Phys. B* **640**, 331 (2002).
- [25] K. Golec-Biernat and M. Wusthoff, *Phys. Rev. D* **59**, 014017 (1998).
- [26] H. Kowalski, L. Motyka, and G. Watt, *Phys. Rev. D* **74**, 074016 (2006).
- [27] H. Kowalski and D. Teaney, *Phys. Rev. D* **68**, 114005 (2003).

- [28] C. Marquet, Robert B. Peschanski, and G. Soyez, *Phys. Rev. D* **76**, 034011 (2007).
- [29] D. Kharzeev and K. Tuchin, *Nucl. Phys. A* **770**, 40 (2008).
- [30] D. McGlinchey, A. D. Frawley, and R. Vogt, *Phys. Rev. C* **87**, 054910 (2013).
- [31] D. E. Kharzeev, E. M. Levin, and M. Nardi, *Nucl. Phys. A* **730**, 448 (2004).
- [32] A. Frawley, T. Ullrich, and R. Vogt, *Phys. Rep.* **462**, 125 (2008).
- [33] N. Brambilla *et al.*, *Eur. Phys. J. C* **71**, 1 (2011).
- [34] Z. B. Kang, Y.-Q. Ma, and R. Venugopalan, *J. High Energy Phys.* **01** (2014) 056.